Open Journal of Geology, 2026, 16(7), 431-449
https://www.scirp.org/journal/ojg
ISSN Online: 2161-7589
ISSN Print: 2161-7570

Niou Gold Deposit Structural Framework, Goren Belt, West African Craton

Yacouba Ouedraogo[1,2]*, Hermann Ilboudo[1,2], Wilfried Antoine Bassou Toe[1,2], Séta Naba[1,2]

[1]Laboratoire Géosciences et Environnement (LaGE), Université Joseph KI-ZERBO, Ouagadougou, Burkina Faso
[2]Département des Sciences de la Terre, Unité de Formation et de Recherche en Sciences de la Vie et de la Terre, Ouagadougou, Burkina Faso
Email: *yacouba.ouedraogo@ujkz.bf

How to cite this paper: Ouedraogo, Y., Ilboudo, H., Toe, W.A.B. and Naba, S. (2026) Niou Gold Deposit Structural Framework, Goren Belt, West African Craton. *Open Journal of Geology*, **16**, 431-449.
https://doi.org/10.4236/ojg.2026.167022

Received: June 15, 2026
Accepted: July 27, 2026
Published: July 30, 2026

Abstract

Niou gold deposit is open-pit mine located in the southwestern portion of Goren segment within Boromo greenstone belt, one of Burkina Faso Birimian greenstone belts that hosts world-class gold deposits. The Goren segment, Borom-Goren belt northeastern part, is one of Burkina Faso birimian formations. This area was affected by multiple deformations and hydrothermal events in Paleoproterozoic. The structural and stratigraphic complexity of the sector requires detailed mapping to constrain the primary controls gold mineralization. Open pit mapping at 1:100 scale, combined with macroscopic logging of drill core representing 6 holes and field mapping, allowed identification of several lithotypes, including: metaandesite, metabasalte and metadiorite, metagabbro dykes, quartz veins with sulfides, chlorite, biotite, quartz carbonate veins. Airborne geophysical imagery interpretation combined with field measurements reveals two sub-meridional (NNW-SSE) shear zones parallel in deposit southern part, which bend to E-W in the eastern portion, where they accommodate mineralized quartz veins, underlying by penetrative foliations and crenulation cleavage. Structural analysis reveals two main deformation phases: 1) an early phase D_{1Ni} responsible for penetration foliation S_{1Ni} dipping to NE or SW, and 2) a shortening event associated with localized shear zones producing crenulation cleavage with NW and SE vergence and NNE-SSW S_{2Ni} schistosity. Dominant hydrothermal alteration styles include carbonation, chloritization, silicification and sulfidation underlying biotite. These combined geological, structural and textural observations indicate that gold deposition at Niou was controlled by the interplay between progressive deformation, lithological contrasts, and multiple episodes of hydrothermal fluid flow, like many other deposits described in the Birimian of West Africa.

Keywords

Niou, Goren, Gold Deposit, Shear Zone, Structural Control

1. Introduction

The Boromo-Goren belt is one of the metalliferous belts of Burkina Faso (**Figure 1**), renowned for its mining potential [1] [2] within the Leo Ridge of the West African Craton (WAC). This craton is rich in mineralization diversity [3]-[6], the majority of which was formed during Eburnean orogeny between 2.2 and 1.8 Ga [7]-[9]. This volcano-sedimentary belt accommodates various intrusions, all of which are organized according to a linear orientation, imposed by polycyclic granitic masses emplacement [10] and a regional shortening [7] [11]. These syn and post-magmatic tectonic phenomena channeled fluid movement responsible for diversity of mineral deposits [5] [6] [8] [12]-[15]. Several mineral deposits have been subject to scientific studies, highlighting their lithostructural and geological characteristics: Larafella [16], Taparko [17]; Essakane [18], Youga [19], Yaramoko [20], Nassara [21], Gaoua [21] [22], Bomboré [23], Inata [24] [25], and Mana [12] [14] are all listed in geoscientific annals (**Figure 2**). However, Niou gold deposit, opened since May 2025, is not yet recorded in geoscientific record. While structural control seems evident, lack of understanding of spatial relationships between structural dynamics and mineralization explains numerous failures recorded during nearby exploration drilling. This study clearly establishes these relationships for better optimization of grade control drilling.

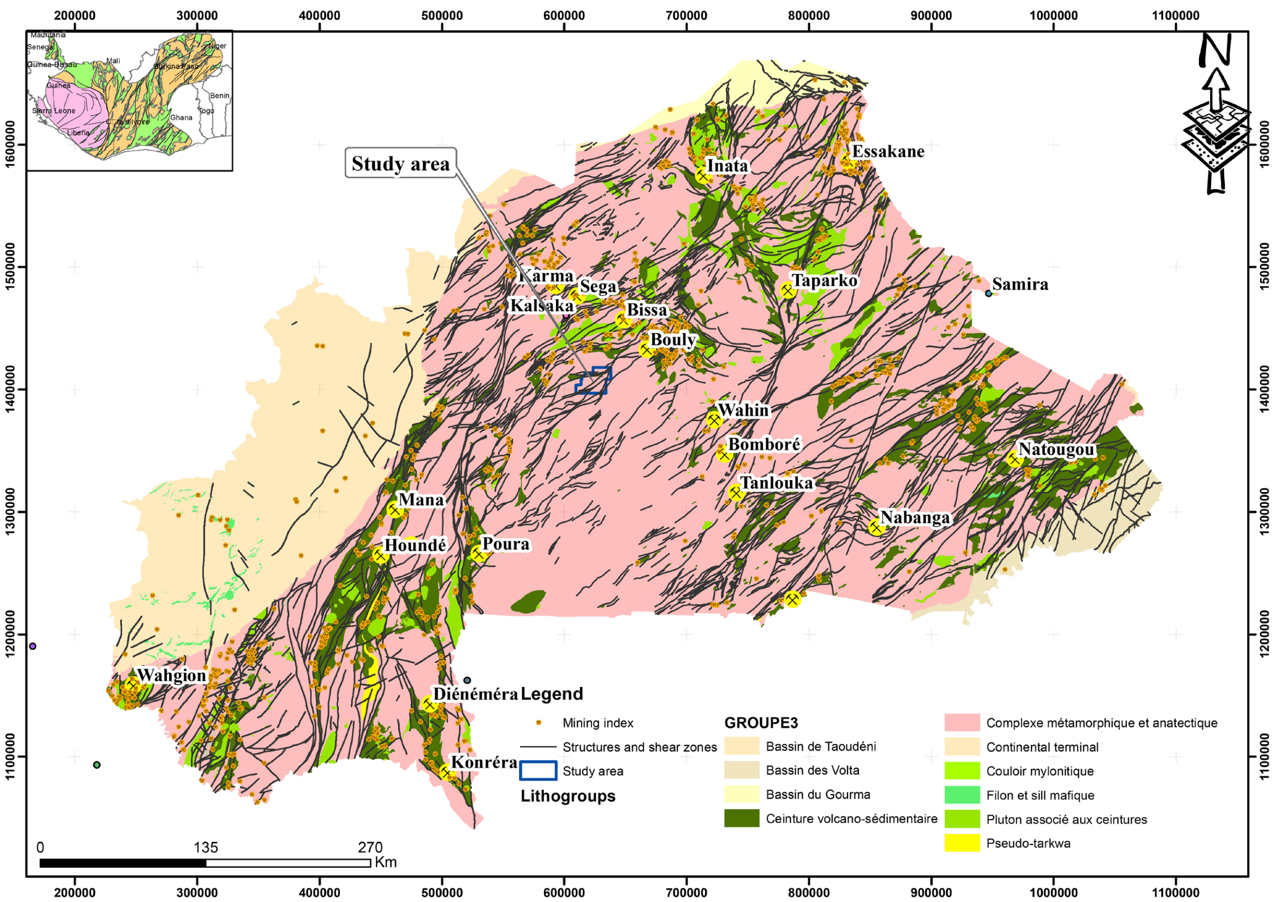

Figure 1. Lithostructural map showing gold deposit locations and advanced project and occurrence minerals.

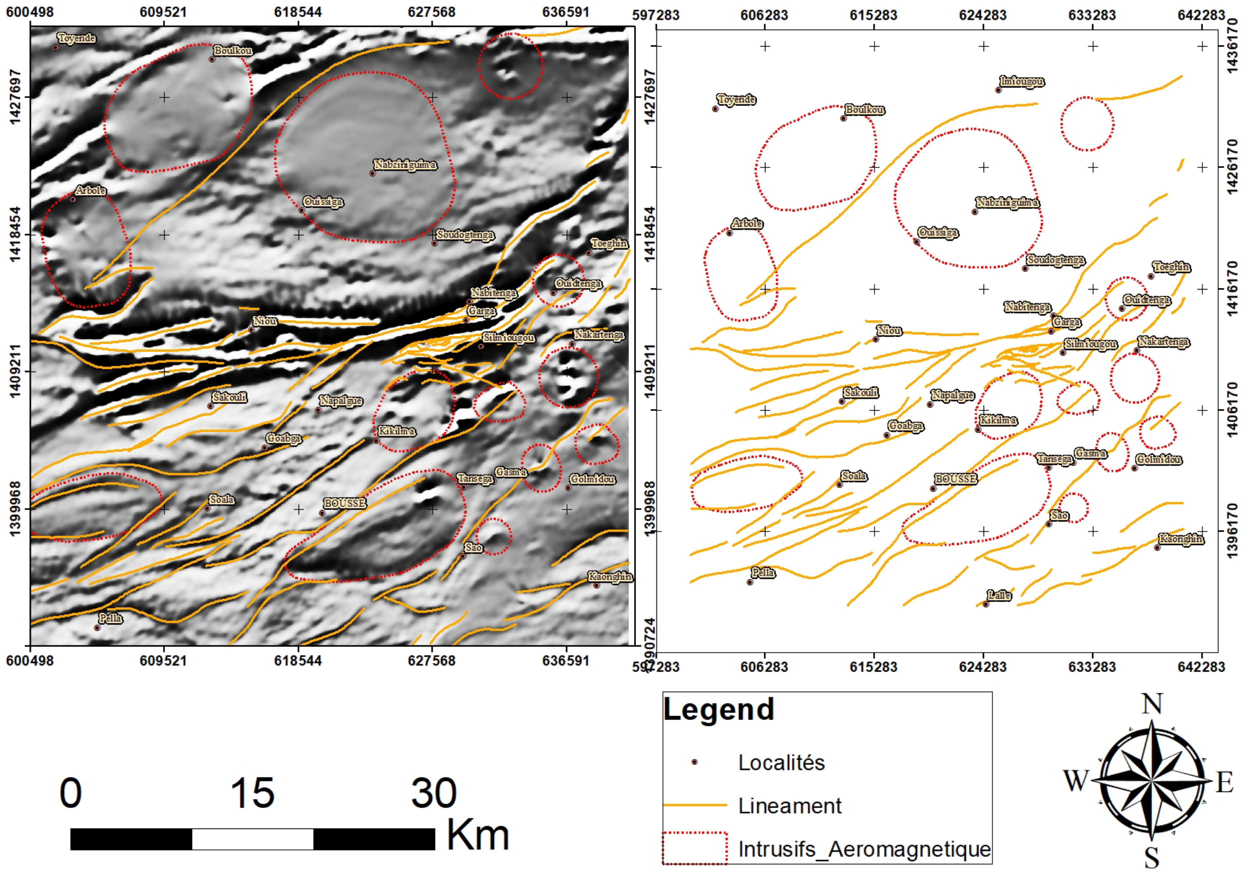

Figure 2. Interpretative structures based on fields structures showing both NNE-SSW shears zones and E-W later shears zones.

2. Geological Settings

Geological study area is part of Goren district one, which is northern extension of Boromo-Goren greenstone belt (**Figure 1**). This regional extension belt continues into NE Ghana to form the Lawra belt [8] [13]. Geological formations that constitute it form a sequence of volcanic and volcanosedimentary rocks cut by syn- and post-tectonic granite intrusions [8] [26]-[29]. This diverse plutonism results in a disturbance of schistosity orientation and transcurrent structures formation perceptible above belt zone, particularly in Sabce corridor [7] [30]. Previously, structural studies [2] [8] [30] identify three phases (D1, D2, D3) in Goren segment and, by extension, in the Niou sector. Early episod deformation, D1, corresponds to collisional tectonics between Congo Craton and West African Craton, characterized in Goren zone district by isoclinal folds synchronous with epi-to mesozonal metamorphism [30]. Second episode D2 and late episode D3 operate within a transcurrent tectonic regime linked to the activity large shear zones, predominantly coaxial for D2 and rotational for D3 [2] [30]. Shear zones worldwide are known to be orogenic gold remobilization drivers [31] [32]. Silmiougou shear zone, an integral part of our study area, is located within Goren shear deformation structures. It was revealed thanks to the structural measurement campaign carried out during field mapping and airborne imagery interpretation (**Figure 3**). This shear zone is a structural interference zone carried by two large shear corridors: the first oriented NE is early and has interfered with the second oriented E-W.

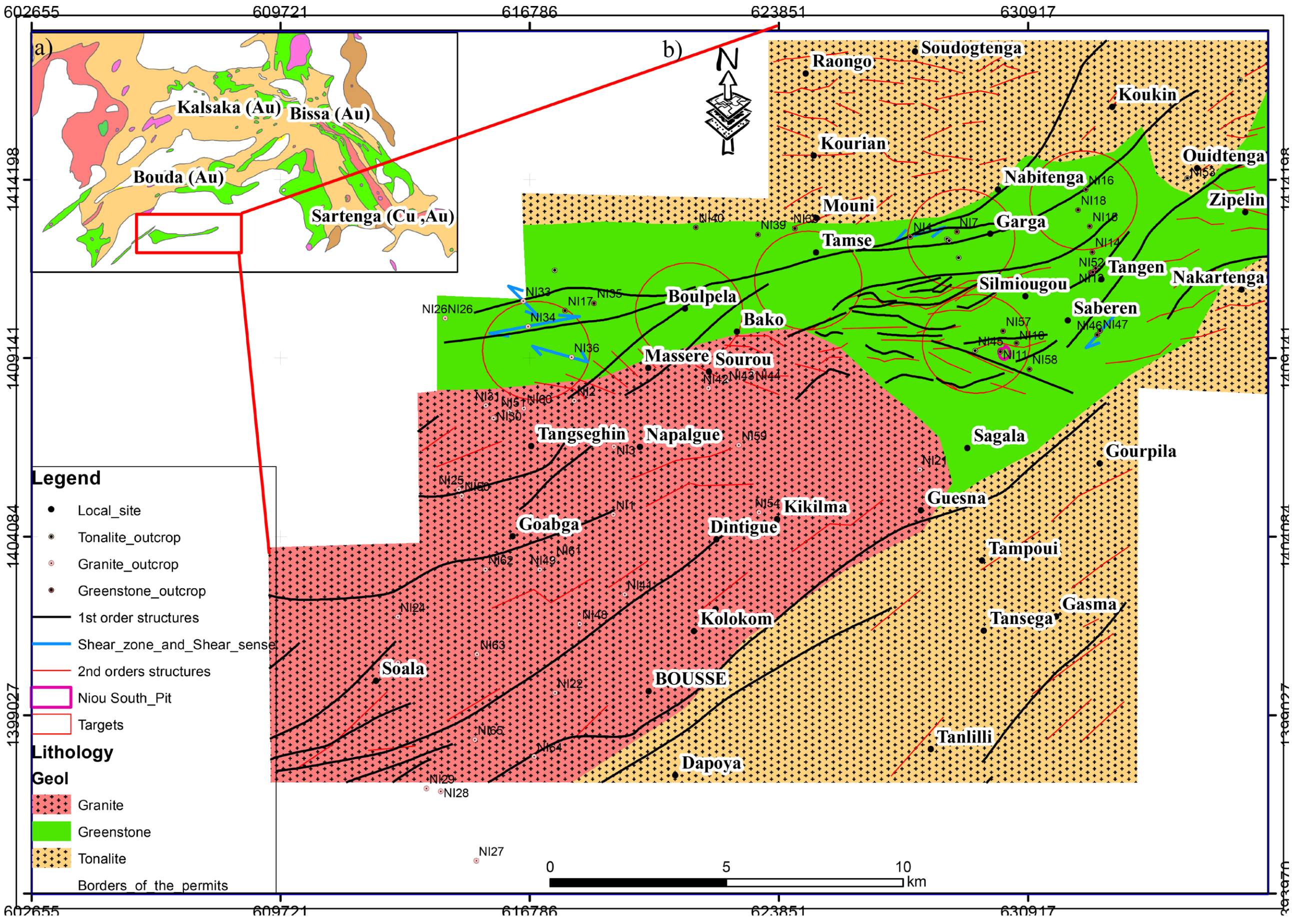

Figure 3. Study area lithostructural maps. (a) Boromo-Goren greenstones belts showing gold deposit. (b) Niou lithostructural map showing shears zones and deposit location.

This tectonic configuration imprints a penetrating foliation/schistosity into the host formations of the Niou gold mineralization. This planar fabric is disrupted by the late-stage calc-alkaline plutonism of the granodiorite in the middle sector, shaping the bedrock into a ductile-brittle structure [28]. This disruption is responsible for the micro-folding of the schistosity and local strike-slip faults directly above the shear zones.

3. Methodology

This study was based on a field mapping campaign and drill core examination. Systematic mapping around NordGold mining property was carried out in two stages: 1) fieldwork, which consisted of core examination preceded by mapping: first regional mapping and then mapping within the mineralized pits. This stage aimed to better understand local geological environment and update available maps, which are not very precise, likely due to the scales of investigation. Drill cores logging supports the preliminary results obtained in the field and helps define the spatial relationships between them. Furthermore, it allows detection of structures deformation in order to characterize the mineralization and its link to other geological phenomena, such as hydrothermal fluid circulation.

Airborne geophysical first vertical derivate imagery interpretation combined with fields measurements helped to define local shear zones and intrusion area. Final image provided by nordgold was used to plot structural field measurement. Shear zone interpreation based on the first vertical derivate map combined with Ouagadougou leaf lithostructural maps.

2) Laboratory work consisting of 18 related to 6 drill holes and thin sections examination prepared using a metallographic microscope at the Geosciences and Environment Laboratory (LaGE) of the Earth Sciences Department at Joseph KI-ZERBO University. This laboratory is equipped with a Nikon Eclipse 50i POL microscope, coupled with a camera, operating in transmitted and reflected light. The microstructural petrographic study and associated metallography were also carried out in this laboratory. This was necessary for the description of the lithologies, the determination of hydrothermal mineral phases, and the microstructural analysis.

4. Results

4.1. Locals Mains Structures

Six (6) planar deformation structures were mapped and measured: foliation (S_{1Ni}), schistosity planes (S_{1Ni}), fractures and fault planes (Fr_{Ni}), folded structures (S_{2Ni}), veins (V_{nNi}), and veinlets and shear planes (C_{nNi}).

4.1.1. Foliation and Schistosity

They are visible in metavolcanic rocks as elongated mounds describing broad NE-SW to E-W trending shears zones and are marked by fine hornblende needles and by the stretching of quartz-feldspathic minerals (**Figure 4(a)**). At outcrops, the foliation planes overlap with the schistosity planes, which break into very tight bundles, particularly in areas of high deformation intensity (**Figure 5(a)**). Due to the local character and similar orientation of these two planes (foliation and schistosity), they are associated in the Niou area.

This local structure, combined with relative chronology, has led to Niou schistosity/foliation being designated S_{1Ni}. S_{1Ni} exhibits an almost ENE-WSW trend with a mean angle of 256˚ and a dip of 50˚ to the north (**Figure 6(b)**). The fine foliation is also marked by the alignment of thin pyrites disseminated parallel to this plane. The planes of these pyrites are slightly flexed due to the behavior of the shear bands and mark synschisteux (C/S) shear planes (**Figure 4(b)**).

4.1.2. Fault and Fractures

Fracture and fault planes (Fr_{Ni}) intersect the foliation/schistosity planes (S_{1Ni}) perpendicularly. Felsic lithotypes are marked by local transpessionnel fault, forming shear markers within these formations. In some areas, fractured blocks are displaced, and fault planes are exposed (**Figure 5(b)**). These fractures contain veins and Carbone-quartz veinlets, and conjugate faults are visible, indicating a sinistral strike-slip movement detectable from their interpretation (**Figure 5(b)**). Chronologically, the fault planes and fractures after the foliation/schistosity and after crenulation cleavage stage are designated S_{3Ni}.

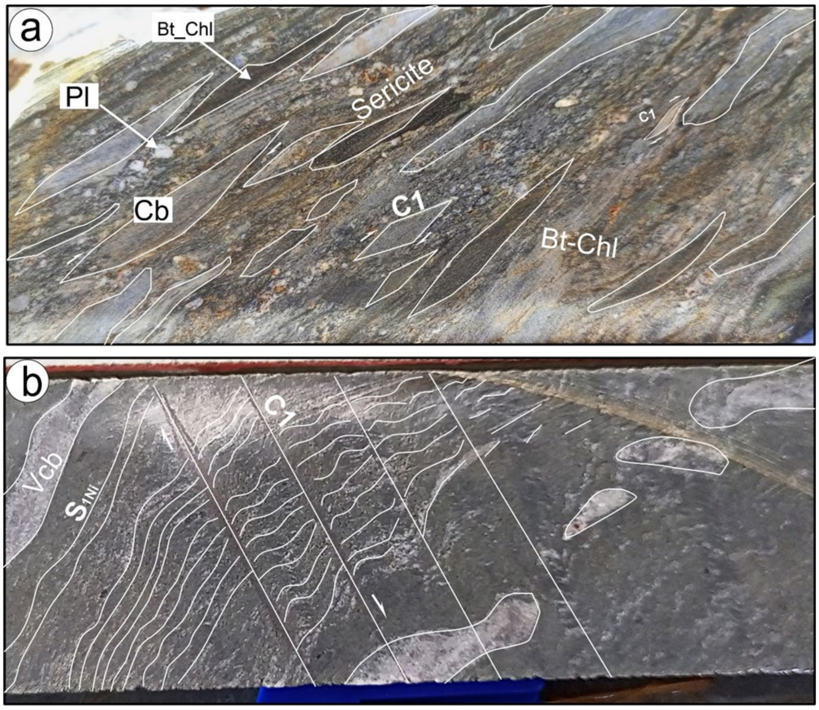

Figure 4. Niou main structures (a) Foliation in metadiorite underling flattening and elongation of quartzofeldspar minerals; (b) S_{1Ni} foliation taken up by C_1 shear planes creating a flexure of the foliation. Note the sulfides disseminated in the plane of the S1Ni foliation. Bt: Biotite; Chl: Chlorite; Cb: Carbonates; C_1: 1st order shear plan 1; Pl: Plagioclase; Vcb: Veine de carbonate; S_{1Ni}: 1st order Niou schistosity plane.

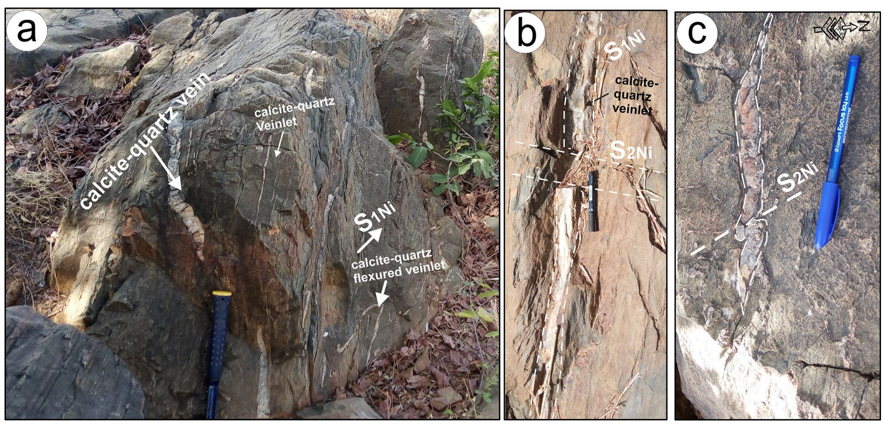

Figure 5. Schistosity planes and veinlets of the Niou zone. (a) S_{1Ni} schistosity developed in a metalave with intercalations of slightly brecciated hematized quartz veins concordant with the S1Ni associated with sterile calcite veins; (b) Carbonate-quartz vein concordant with the S_{1Ni} schistosity taken up by the S_{2Ni} fracture schistosity; (c) Microfolded carbonate-quartz veinlet of quartz concordant with the S_{1Ni} foliation and taken up by the S_{2Ni} crenulation. S_{1Ni}: 1st order Niou schistosity; S_{2Ni}: 2nd order Niou schistosity.

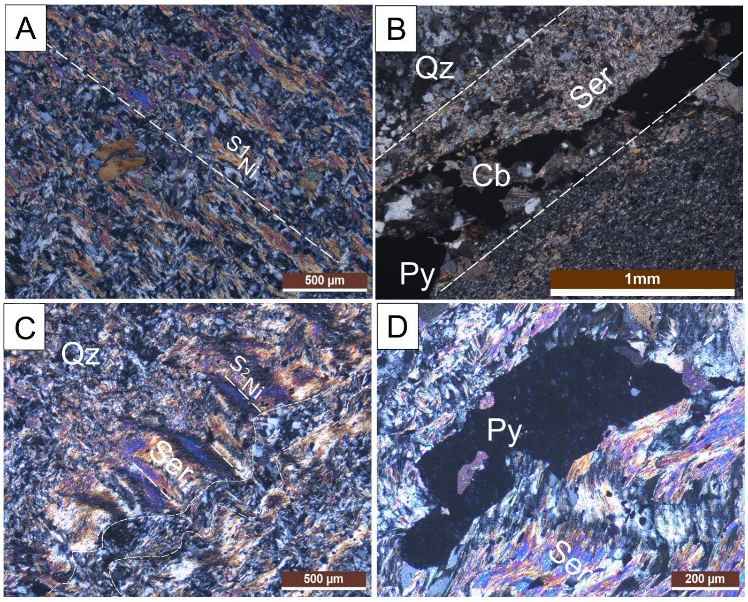

Figure 6. Microstructures associated with the Niou formations: (a) Marked flow schistosity, with minerals aligned parallel to the S_{1Ni} foliation planes in a subgrained recrystallized quartz matrix; (b) Quartz-carbonate and sulfide veins parallel to the S_{1Ni}; (c) S_{2Ni} retracing the flow schistosity planes by microfolding them. Note that the microfold axes are filled with small recrystallized quartz crystals and the veins with microfolded quartz; (d) Slightly fractured pyrite crystal that underwent rotation during deformation; D_{2Ni} microfolding the flow schistosity planes, filled with quartz crystals. Bt: Biotite; Chl: Chlorite; Cb: Carbonates; Qz: Quartz; Py: Pyrite; Ser: Sericite; S_{1Ni}: Niou schistosity 1; S_{2Ni}: Niou schistosity 2; D_{1Ni}: 1st stage of Niou deformation event; D_{2Ni}: 2nd stage of Niou deformation event.

4.1.3. Veins and Veinlets

Veins and veinlets in the Niou area are predominant in volcanic units and rarely in metasedimentary units. Two vein and veinlet types are described at Niou zone: veins concordant with the schistosity (V_{1Ni}) and veins discordant with the schistosity (V_{2Ni}). The first vein generation is more deformed, sulfide-rich and developing boudinage and slow folding hosted in shears zone and look like shears veins. V_{1Ni} veins are intercalated between foliation and schistosity planes and are predominantly filled with quartz, quartz-carbonates, or carbonates. This vein type-oriented 256˚ and dipping to 50˚ in E-W (**Figure 6(c)**) structure domain exhibits ferrous oxide with box-works traces and is highly mineralized (**Figure 5(a)**). They are characterized by traces of breccia and exhibit gold-bearing sulfides at their walls, located within a hermitized gangue (**Figure 7(a)**). In metasedimentary units, they form curled quartz pebbles in the form of sigmoid lenses.

V_{2Ni} veins developed into late fractures, discordant to schistosity S_{1Ni} planes and slightly microfolded in places (**Figure 7(a)**). These veins lack any associated gold mineralization, which is likely subsequent to the mineralization episode.

4.1.4. Folds Structures

Folded structures are mostly crenulation cleavage and micro-folded quartz-carbonate veinlets. Crenulation cleavage plans (S_{2Ni}) form axial planes to S_{1Ni} schistosity micro-folding. Their planes as well look like fracture planes, which are perpendicular S_{1Ni} schistosity planes (**Figure 5(a)**, **Figure 5(b)**, **Figure 7(b)**). S_{2Ni} plane is sub-horizontal trending (N85˚) and dipping slightly to NW and SE (50˚).

Folded structures are also represented by micro-folded carbonate-quartz veinlets (**Figure 5(c)**). At the microscopic scale, crenulation cleavage is marked by flexure sericite flakes. These flexure sericite flakes are micro-folded by S_{2Ni} cleavage crenulation (**Figure 7(a)**). S_{2Ni} microfold axes are filled with small, recrystallized quartz crystals and are crossed by a vein of micro-folded quartz. Slightly fractured pyrite crystals undergo rotation during the late deformation associated with the crenulation cleavage (**Figure 7(b)**, **Figure 8(a)**).

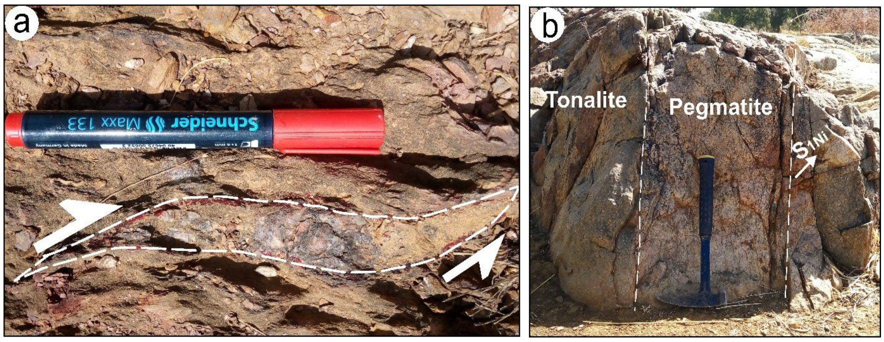

Figure 7. Ductile and brittle deformation structures. (a) Quartz lens subjected to dextral shearing in a metapelite. (b) Pegmatite vein concordant with S1Ni in a tonalite laminated parallel to the tonalite lamination direction.

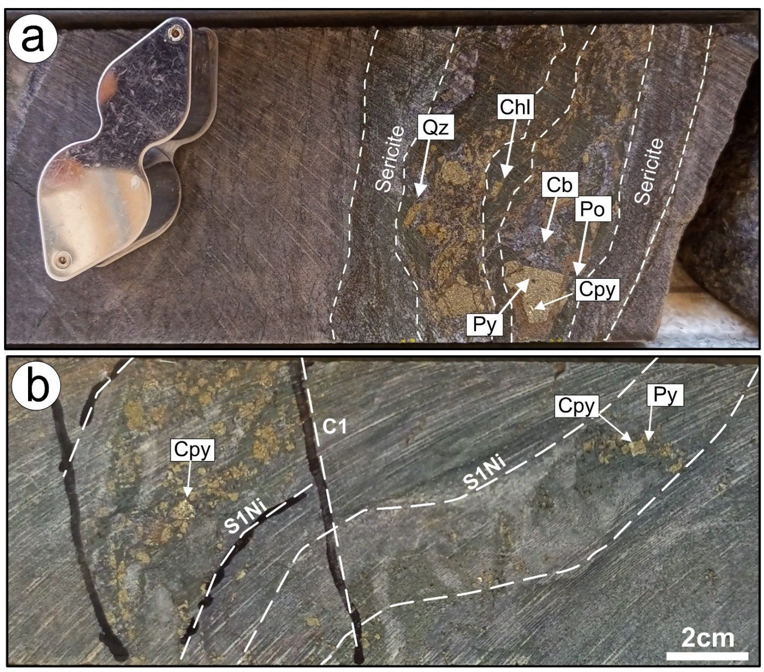

Figure 8. Photographic illustrations of sulfides hosted within local bands of locally flexed S/C and SNi structures. (a) Sulfides hosted within a localized band of silicic carbonate alteration superimposed by chloritization and sericitization; (b) Lenses filled with pyrite containing chalcopyrite inclusions embedded in a chloritic silico-carbonate matrix. Bt: Biotite; Chl: Chlorite; Cb: Carbonates; Qz: Quartz; Cpy: Chalcopyrite; Po: Pyrrhotite; Py: Pyrite; Ser: Sericite. S_{1Ni}: Niou schistosity 1; S_{2Ni}: Niou schistosity 2.

4.1.5. Pegmatites Veins

Pegmatite dikes form intruded unit across tonalitic areas around Niou NW portion. It looks like tonalites and granites lamination planes and are parallel to this direction (**Figure 9**).

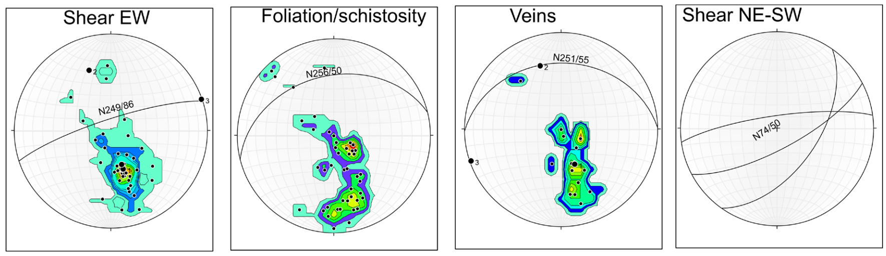

Figure 9. Stereoplot of structural measurements of shear planes of foliation/schistosity and veins.

4.2. Structural Control on Gold Mineralization

These are the quartz and quartz-carbonates' veins and veinlets, the local shear bands, and the planes of schistosity.

4.2.1. Shears Bands: C_{Ni}

C_{Ni} shear bands are localized areas characterized by intense deformation that undermines the rock early characteristics, such as minerals and rocks textures. Shears zones or shears bands delineate S_{1Ni} schistosity planes portions, where they form synschisteux C/S shear structures trending to N249˚ and dipping to 86 over 71 measurements (**Figure 6(a)**) in E-W part of deposit and trend to 74 dipping to 50 in NE part (**Figure 6(d)**). These shear corridors exhibit porosity and permeability, serving as receptacles for mineralizing fluids organized into sygmoidal veins in echelon form or into veins and veinlets concordant with these shear planes. Furthermore, the walls or contact zones of these shear bands also constitute prime targets for disseminated mineralization subsequently transposed into the foliation planes.

4.2.2. Schistosity

The schistosity planes exert true control over the Niou Gold mineralization. These planes drain a foliation of mafic minerals (hornblende and biotite) in their direction, upon which elongated sulfides develop. These sulfides, composed mainly of pyrite, are highly gold-mineralized. They are associated with strong pervasive silicification and chloritization and sericitization parallel to S_{1Ni} (**Figure 8**).

4.2.3. Crenulation Cleavage

Crenulation schistosity overlays the structures of compositional S_{1Ni} foliation/ribboning schistosity, forming crenulated cleavages in volcanic and metapelitic units (**Figure 5(a)**, **Figure 9**). In places, these cleavages form centimeter or millimeter-scale folds in metabasaltic and metaandesitic units. Their micro hinges are the preferred sites of concentration of gold-bearing sulfides, which are predominant in metaandesitic units (**Figure 9**).

5. Discussion

5.1. Structural Evolution

Based on field observations and structural analysis described above, volcanics rock types, intrusive units, and metasediments exhibit progressive and polyphasic deformation. Indeed, at least three deformation increments can be linked to the structural events in the Niou area: two ductile deformation events (D_{1Ni}, D_{2Ni}) and one brittle deformation event (D_{3Ni}). **Table 1** incorporates the structural features observed at the outcrop scale and on drill cores to define a nomenclature specific to each increment of deformation. Structural fabrics are collectively designated S_{1Ni}, S_{2Ni}, V_{1Ni}, V_{2Ni}, C_{1Ni}, C_{2Ni}… D_{1Ni} deformation increment is characterized by penetrative foliation and a tight-packed S_{1Ni} schistosity development. In localized first-order shear zones, this foliation tends to mylonitize when it overlies volcanic units. Under these rheological conditions, the rock progressively acquires mylonitized structures (protomylonites, ultramylonites), preferentially within the volcanic units, by creating a structure favorable to the flow of mineralizing fluids [12] [31]-[35].

Table 1. Summary table outlining the events and associated structural elements.

Deformations events		Associated structures
Ductile deformation	**D_{1Ni}**	S_{1Ni}
		S_{1Ni}/C_{1Ni}
		V_{1Ni}
	D_{2Ni}	S_{2Ni}
		S/C_{2Ni}
		V_{2Ni}
Brittle deformation	**D_{3Ni}**	V_{3Ni}
		Fr_{Ni}

S_{1Ni}: Niou schistosity 1; S_{2Ni}: Niou schistosity 2; D_{1Ni}: 1st stage of Niou deformation event; D_{2Ni}: 2nd stage of Niou deformation event; D_{3Ni} 3rd stage of Niou deformation event; S/C_{1Ni}: 1st order synschitosy shear plan; S/C_{2Ni}: 2nd order synschitosy shear; plan P_{1Ni}: Niou 1st stage fold; V_{1Ni}: Niou 1st vein and veinlets order; V_{2Ni}: Niou 2nd vein and veinlets order; V_{3Ni}: Niou 3rd vein and veinlets order; plan P_{2Ni}: Niou 2nd stage fold.

S_{1Ni} schistosity concordant veins and veinlets (**Figure 10(a)**, **Figure 10(b)**) show their emplacement in a context of ductile deformation, particularly in a shear deformation context (**Figure 10(c)**), and are interpreted as having been formed by sliding involving a shear component [36] [37]. Micro folded veinlets and boudinage veins are therefore interpreted as entrainment folds due to S_{1Ni} effect, along a slip plane (**Figure 10(d)**). Localized shear bands materialized in the volcanic units could act as slip planes favorable to the formation of these microfolds and as sites for trapping mineralizing fluids [38].

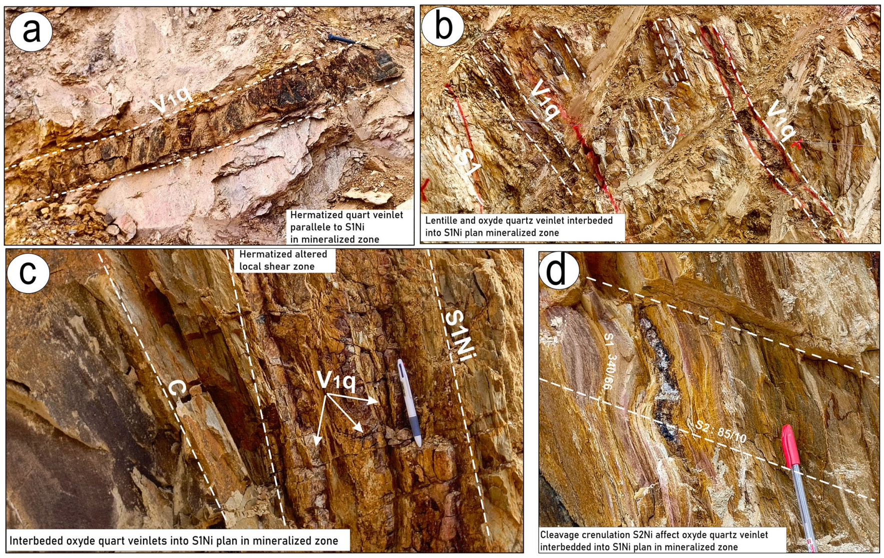

Figure 10. Deformation structures associated with gold mineralization. C: Shear; plan V1q: 1st order of quartz vein and veinlets; S1Ni: 1st order of Niou schistosity.

Subvertical dipping schistosity and associated frustrated foliation represent subvertical shortening and elongation effect. However, the obliquity between the S_{1Ni} schistosity in the central E-W sector trending to SW-NE as 249˚ and still straightens 86˚ and the NE domain trending to 74˚ and dipping to 50˚ could represent the relationships between an S-plane and a C-plane, which can be interpreted as evidence of dextral strike-slip faulting [28] [30]. Z-folded veinlets predominantly, interpreted as intrafoliar folds between shear bands, are consistent with dextral strike-slip faulting that likely initiated during D_{1Ni} and continued progressively during D_{2Ni}. This S_{1Ni} rotational deformation-type strike-slip faulting can be interpreted as representing an increment of dextral strike-slip shear. In summary, during the D_{1Ni} deformation event, the lithological units of the Niou sector located in the E-W, NE-SW structural interference zone were probably affected by shortening accompanied by subvertical stretching and locally associated with the beginning of dextral strike-slip movement.

D_{2Ni} deformation event is marked by the development of Z-folds accompanied by S_{2Ni} crenulation cleavage. Z-folds generation is evidenced by folded veinlets trapped between local shear bands, justifying their early appearance relative to this episode. Microfold hinges formed from quartz-carbonate-sulfide-filled veins located within these shear bands perfectly illustrate the D_{2Ni} event, which reworked these early D_{2Ni} structures. Folded structures generation is interpreted as interference result E-W local shear zones abutting early local NE-SW shear structures zone. In places, strike-slip structures are evidenced by regional-scale transgressional faults detectable through the interpretation of airborne geophysical imagery. [39] interprets these increments of interfering deformation as an anastomosing transpressure network conferred by a three-dimensional partitioning of progressive transgressional deformation and interactions between local shear zones. This could explain the presence of both dextral and sinistral strike-slip faults in the Niou area.

The V_{2Ni} veins are related to the D_{2Ni} deformation event. These veins are generally barren and could be the product of quartz exudation from intrusive rocks and volcanic rocks [40] rather than the hydrothermal activity with which the mineralized veins are associated. The absence of sulfides within these veins and of alteration at the walls supports the hypothesis of a metamorphic source. Finally, the D_{3Ni} brittle event has only a weak influence on the geometry of the lithological units and their assemblage, and on the structural control of the mineralized zones by late-onset fractures and sinistral strike-slip faults.

5.2. Mineralization Structural Control

Within the Silmiougou shear zone, three major deformation phases have been defined in this mineralized corridor. The first deformation phase, D_{1Ni}, is a shear deformation with the same characteristics as the larger-scale D_2 phase defined by [28] and [30]. D_{2Ni}, a ductile-brittle tectonic deformation, is comparable to D_3, defined by the same authors as a semi-ductile deformation associated with sinistral shear, orienting the structures to NW-SE.

Hydrothermal alteration phases that affect the host rocks can be correlated with mineralization and deformation episodes defined in the Silmiougou shear zone. During the D_{1Ni} shear deformation, strong biotitization is associated with this phase, creating a foliation characterized by the alignment of biotite crystals along this plane. Biotitization is also vein-like and is associated with veins and veinlets of mineralized sulfides oriented parallel to the point of view of S_{1Ni}.

Associated metamorphism creates a pseudomorphosis, and a new mineral formation is acquired. Ferromagnesian and quartz-feldspathic minerals metamorphose into chlorite and ferromagnesian oxides, respectively, associated with secondary quartz, and are drained in planes parallel to subparallel to the S_{1Ni}. Biotite, chlorite, and carbonates constitute precursor minerals for pyritization and gold mineralization phases. This result is like what some authors [21] [41] have proposed for the El Callao deposit in the Guiana craton and the Nassara deposit in the West African craton, respectively. The shear deformation D_{1Ni} is followed by a second ductile to brittle ductile deformation D_{2Ni}. It will be responsible for the acquisition of locally folded S_{2Ni} structures formed by crenulation cleavages sub-orthogonal to foliation and shear schistosity. It microfolds the mica flakes that trap pyrite crystals at the micro hinges of the crenulation schistosity. This deformation is also responsible for the opening of sub orthogonal microfractures in plagioclase phenocrysts, which fill with white mica, and for the formation of fills filled with these sulfides, which are common to many deposits already characterized in the Man/Leo ridge: the Loulo deposit in Mali [42], the Mana deposit [12], and in particular the Nassara deposit [21], Kiaka deposit [33], and the Bissa deposit [43].

Pervasive alteration synchronous with mineral creep of the D_{1Ni} deformation consists of predominant chloritization in mafic units and predominant sericitization in intrusive units. These different alterations are locally superimposed by either silicification or carbonation, sometimes saussuritization or even sericitization. Biotitisation and chloritization are the early stages of pyritization, which originates from iron leached by ferromagnesian minerals on the one hand, and from ferriferous carbonates, which, along with sulfur, contribute to the strong crystallization of sulfides in almost all the deposit's lithologies, on the other. Chloritization and sericitization are considered early alterations indicating the beginning of hydrothermal fluid circulation [44] and spatially marking the main drainage channels typically reused by mineralizing fluids. This interpretation is similar to that proposed by [41] [21] according to which iron carbonates constitute the privileged zones for the precipitation of pyrites.

In shear zones, gold mineralization is generally accepted as continuous at depth and is linked to fluid circulation from ductile to brittle stages [32] [41]. Early fluid circulation, resulting in quartz, carbonates, and pyrites in veins/veinlets crystallization at Niou zone, is thought to be fluids collected along the rocks traversed during the D_{1Ni} deformation phase, from ductile to brittle stages (**Figure 10**). It has been shown that during their ascent, fluids interact with rocks they pass through, thereby extracting most of the metals, which become complex as ions in solution and precipitate in the various traps within the ductile-brittle to brittle layers [44] [45]. It has also been shown that tholeiitic basalts are fertile rocks for gold mineralization from the moment of their emplacement [12] [21] [41]. This would prove that the metavolcanic rocks (meta-andesite and metabasalt) of Niou were fertile rocks at the time of their accretion and that this primary gold would be remobilized by the fluid during its ascent by metasomatic phenomena to manifest itself in the form of veins/veinlets of quartz-white mica-pyrite ± chlorite ± carbonate ± arsenopyrite.

In the West African craton, the most frequent associated sulfides in gold deposits are pyrite, pyrrhotite, chalcopyrite, and arsenopyrite [46]-[55]. These sulfides are typical of orogenic gold deposits. These sulphide's types have been characterized in the Niou deposit. These mineralization pathfinders, disseminated within volcanic rocks and located in quartz and carbonate veins, and controlled by the Silmiougou shear zone and the S_{1Ni} formation, make Niou an orogenic deposit. Furthermore, in these economic deposits, main phase of mineralization is followed by one or more deformation phases where primary gold is remobilized and reconcentrated in the microfractures of the sulfides [17]. In contrast, the shear structure that controls the gold mineralization of Niou is reworked by the D_{2Ni} formation but does not significantly affect the mineralization to the point of remobilizing it, even though it could contribute to a local redistribution of the mineralization in the micro-hinges of the sigmoid veins. This makes Niou a more specific deposit compared to other economic deposits. This D_{2Ni} is comparable to D_{3Na} in the Nassara gold deposit, where the latter does not lead to a remobilization of the mineralization controlled by the D_{2Na} shear structure [21]. These different parameters are summarized in the conceptual model integrating the different lithologies as well as the deformation structures of gold mineralization (**Figure 11**).

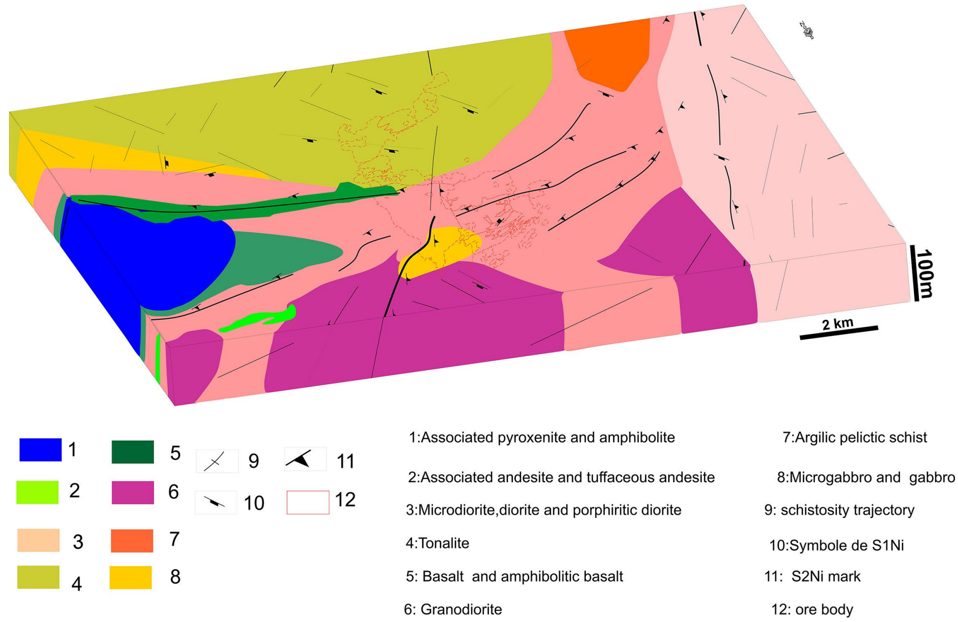

Figure 11. 3D model representing the different deformation structures associated with the Niou deposit.

6. Conclusion

Niou gold deposit exhibits a strong structural imprint. Mineralization is primarily controlled by local shear bands with a major subvertical orientation, although these bands bend in the western sector. Quartz-carbonate shear veins and extension veins concordant with the S_{1Ni} schistosity represent the preferential sites for gold crystallization, demonstrating strong structural control of the schistosity over mineralization. These characteristics show similarities with known orogenic gold deposits in the West African Craton, the Abitibi region, and various Archean and Paleoproterozoic gold-bearing cratons. This study highlights the Niou gold deposit and contributes to our understanding of the West African craton's mineral portfolio, although further studies on the evolution of the hydrothermal system are needed for a better understanding of this deposit, which is currently being mined in the Goren segment.

Acknowledgements

The authors would like to thank the Projet d'Appui à l'Enseignement Supérieur (PAES) and the mining company NordGold Bissa for their support of this study. The Agathe project is also gratefully acknowledged for its scientific support.

Author Contributions

Conceptualisation: Yacouba Ouedraogo, Hermann Ilboudo, Wilfried AB Toe and Séta Naba.

Methodology: Yacouba Ouedraogo, Wilfried AB Toe, Séta Naba and Hermann Ilboudo.

Sofware: Yacouba Ouedraogo and Séta Naba.

Writting—review and editing: Yacouba Ouedraogo, Hermann Ilboudo and Wilfried AB Toe.

Supervision: Hermann Ilboudo, Séta Naba and Wilfried AB Toe.

Funding: Yacouba Ouedraogo, NordGold and Agathe project.

All authors have read and agreed to the published version.

Conflicts of Interest

The authors declare no conflicts of interest regarding the publication of this paper.

References

[1] Napon, S. (1988) Le gisement d'amas sulfurés (Zn-Ag) de Perkoa dans la province du Sangyé (Burkina Faso Afrique de l'Ouest): Cartographie, étude pétrographique, géochimique et métallogénique. Master's Thesis, University de Franche-Comté.

[2] Castaing, C., *et al.* (2003) Notice explicative de la Carte géologique du Burkina Faso à 1/200,000. Bureau de Recherches Géologiques et Minières.

[3] Markwitz, V., Hein, K.A.A. and Miller, J. (2016) Compilation of West African Mineral Deposits: Spatial Distribution and Mineral Endowment. *Precambrian Research*, **274**, 61-81. https://doi.org/10.1016/j.precamres.2015.05.028

[4] Gaboury, D. (2019) Parameters for the Formation of Orogenic Gold Deposits. *Applied Earth Science*, **128**, 124-133. https://doi.org/10.1080/25726838.2019.1583310

[5] Thébaud, N., Allibone, A., Masurel, Q., Eglinger, A., Davis, J., André-Mayer, A., *et al.* (2020) Chapter 34. The Paleoproterozoic (Rhyacian) Gold Deposits of West Africa. In: *Geology of the World's Major Gold Deposits and Provinces*, Society of Economic Geologists, 735-752. https://doi.org/10.5382/sp.23.34

[6] Masurel, Q., Thébaud, N., Allibone, A., André-Mayer, A., Hein, K.A.A., Reisberg, L., *et al.* (2019) Intrusion-Related Affinity and Orogenic Gold Overprint at the Paleoproterozoic Bonikro Au-(Mo) Deposit (Côte d'Ivoire, West African Craton). *Mineralium Deposita*, **57**, 557-580. https://doi.org/10.1007/s00126-019-00888-2

[7] Lompo, M. (2009) Geodynamic Evolution of the 2.25-2.0 Ga Palaeoproterozoic Magmatic Rocks in the Man-Leo Shield of the West African Craton. A Model of Subsidence of an Oceanic Plateau. *Geological Society, London, Special Publications*, **323**, 231-254. https://doi.org/10.1144/sp323.11

[8] Baratoux, L., Metelka, V., Naba, S., Jessell, M.W., Grégoire, M. and Ganne, J. (2011) Juvenile Paleoproterozoic Crust Evolution during the Eburnean Orogeny (~2.2-2.0 Ga), Western Burkina Faso. *Precambrian Research*, **191**, 18-45. https://doi.org/10.1016/j.precamres.2011.08.010

[9] Perret, J., Thebaud, N., Fougerouse, D., Brochard, C., Hayman, P. and Jessell, M. (2025) Crustal to Microscale Strain Partitioning during Transpression and Control on Ore Formation: Insights from the Paleoproterozoic Séguéla Shear Zone, Southern West African Craton. *Tektonika*, **3**, 127-154. https://doi.org/10.55575/tektonika2025.3.2.108

[10] Ilboudo, H., Sawadogo, S., Kagambega, N. and Remmal, T. (2021) Petrology, Geochemistry, and Source of the Emplacement Model of the Paleoproterozoic Tiébélé Granite Pluton, Burkina Faso (West-Africa): Contribution to Mineral Exploration. *International Journal of Earth Sciences*, **110**, 1753-1781. https://doi.org/10.1007/s00531-021-02039-3

[11] Lompo, M. (2010) Paleoproterozoic Structural Evolution of the Man-Leo Shield (West Africa). Key Structures for Vertical to Transcurrent Tectonics. *Journal of African Earth Sciences*, **58**, 19-36. https://doi.org/10.1016/j.jafrearsci.2010.01.005

[12] Augustin, J. and Gaboury, D. (2017) Paleoproterozoic Plume-Related Basaltic Rocks in the Mana Gold District in Western Burkina Faso, West Africa: Implications for Exploration and the Source of Gold in Orogenic Deposits. *Journal of African Earth Sciences*, **129**, 17-30. https://doi.org/10.1016/j.jafrearsci.2016.12.007

[13] Amponsah, P.O., Salvi, S., Béziat, D., Baratoux, L., Siebenaller, L., Nude, P.M., *et al.* (2016) The Bepkong Gold Deposit, Northwestern Ghana. *Ore Geology Reviews*, **78**, 718-723. https://doi.org/10.1016/j.oregeorev.2015.06.022

[14] Augustin, J. and Gaboury, D. (2019) Multi-Stage and Multi-Sourced Fluid and Gold in the Formation of Orogenic Gold Deposits in the World-Class Mana District of Burkina Faso—Revealed by LA-ICP-MS Analysis of Pyrites and Arsenopyrites. *Ore Geology Reviews*, **104**, 495-521. https://doi.org/10.1016/j.oregeorev.2018.11.011

[15] Grenholm, M., Jessell, M. and Thébaud, N. (2019) A Geodynamic Model for the Paleoproterozoic (ca. 2.27-1.96 Ga) Birimian Orogen of the Southern West African Craton—Insights into an Evolving Accretionary-Collisional Orogenic System. *Earth-Science Reviews*, **192**, 138-193. https://doi.org/10.1016/j.earscirev.2019.02.006

[16] Bamba, O., Beziat, D., Bourges, F., Debat, P., Lompo, M., Parizot, J., *et al.* (1997) Nouveau type de gisement aurifère dans les ceintures de roches vertes birimiennes du Burkina Faso: Les albitites de Larafella. *Journal of African Earth Sciences*, **25**, 369-381. https://doi.org/10.1016/s0899-5362(97)00110-3

[17] Bourges, F., Debat, P., Tollon, F., Munoz, M. and Ingles, J. (1998) The Geology of the Taparko Gold Deposit, Birimian Greenstone Belt, Burkina Faso, West Africa. *Mineralium Deposita*, **33**, 591-605. https://doi.org/10.1007/s001260050175

[18] Tshibubudze, A. and Hein, K.A.A. (2016) Gold Mineralisation in the Essakane Goldfield in Burkina Faso, West African Craton. *Ore Geology Reviews*, **78**, 652-659. https://doi.org/10.1016/j.oregeorev.2015.10.030

[19] Kirk Woodman, K., Baratoux, L., Somda, A. and Siebenaller, L. (2016) The Youga Gold Deposit, Burkina Faso. *Ore Geology Reviews*, **78**, 631-638. https://doi.org/10.1016/j.oregeorev.2015.11.015

[20] Hein, K.A.A. (2016) The Bagassi Gold Deposits on the Eastern Margin of the Houndé Greenstone Belt, Burkina Faso. *Ore Geology Reviews*, **78**, 660-666. https://doi.org/10.1016/j.oregeorev.2015.10.028

[21] Ouiya, P., Siebenaller, L., Salvi, S., Béziat, D., Naba, S., Baratoux, L., *et al.* (2016) The Nassara Gold Prospect, Gaoua District, Southwestern Burkina Faso. *Ore Geology Reviews*, **78**, 623-630. https://doi.org/10.1016/j.oregeorev.2015.11.026

[22] Le Mignot, E., Siebenaller, L., Béziat, D., André-Mayer, A., Reisberg, L., Salvi, S., *et al.* (2017) The Paleoproterozoic Copper-Gold Deposits of the Gaoua District, Burkina Faso: Superposition of Orogenic Gold on a Porphyry Copper Occurrence? *Economic Geology*, **112**, 99-122. https://doi.org/10.2113/econgeo.112.1.99

[23] Zongo GH (2017) Caractérisation du gisement aurifère de bomboré: Pétrographie, géochimie, déformation, altération hydrothermale et minéralisation (Burkina Faso, Afrique de l'ouest). Thèse de Doctorat, Université Joseph Ki-Zerbo Ouagadougou.

[24] Lebrun, E., Thébaud, N., Miller, J., Roberts, M. and Evans, N. (2016) Mineralisation Footprints and Regional Timing of the World-Class Siguiri Orogenic Gold District (Guinea, West Africa). *Mineralium Deposita*, **52**, 539-564. https://doi.org/10.1007/s00126-016-0684-6

[25] Ilboudo, H., Sawadogo, S., Traoré, A.S., Sama, M., Wenmenga, U. and Lompo, M.

(2018) Intrusion-Related Gold Mineralization: Inata Gold Deposit, Bélahourou District, Northern Burkina Faso (West-Africa). *Journal of African Earth Sciences*, **148**, 52-58. https://doi.org/10.1016/j.jafrearsci.2018.05.015

[26] Lompo, M. (1991) Etude geologique et structurale des series birimiennes de la region de kwademen-burkina faso-afrique de l'ouest. Doctoral Dissertation, Clermont-Ferrand 2.

[27] Metelka, V., Baratoux, L., Naba, S. and Jessell, M.W. (2011) A Geophysically Constrained Litho-Structural Analysis of the Eburnean Greenstone Belts and Associated Granitoid Domains, Burkina Faso, West Africa. *Precambrian Research*, **190**, 48-69. https://doi.org/10.1016/j.precamres.2011.08.002

[28] Hein, K.A.A., Morel, V., Kagoné, O., Kiemde, F. and Mayes, K. (2004) Birimian Lithological Succession and Structural Evolution in the Goren Segment of the Boromogoren Greenstone Belt, Burkina Faso. *Journal of African Earth Sciences*, **39**, 1-23. https://doi.org/10.1016/j.jafrearsci.2004.05.003

[29] Hein, K.A.A. (2010) Succession of Structural Events in the Goren Greenstone Belt (Burkina Faso): Implications for West African Tectonics. *Journal of African Earth Sciences*, **56**, 83-94. https://doi.org/10.1016/j.jafrearsci.2009.06.002

[30] Feybesse, J.L., Milesi, J.P., Ouedraogo, M.F. and Prost, A. (1990) La "ceinture" protérozoïque inférieur de Boromo-Goren (burkina faso): Un exemple d'interférence entre deux phases transcurrentes éburnéennes. *Comptes Rendus de l'Académie des Sciences. Série* 2, *Mécanique*, *Physique*, *Chimie*, *Sciences de l'Univers*, *Sciences de la Terre*, **310**, 1353-1360.

[31] Groves, D.I., Goldfarb, R.J., Gebre-Mariam, M., Hagemann, S.G. and Robert, F. (1998) Orogenic Gold Deposits: A Proposed Classification in the Context of Their Crustal Distribution and Relationship to Other Gold Deposit Types. *Ore Geology Reviews*, **13**, 7-27. https://doi.org/10.1016/s0169-1368(97)00012-7

[32] Goldfarb, R.J., Baker, T., Dubé, B., Groves, D.I., Hart, C.J.R. and Gosselin, P. (2005) Distribution, Character, and Genesis of Gold Deposits in Metamorphic Terran. In: Hedenquist, J.W., *et al.*, Eds., *Economic Geology* 100*th Anniversary Volume*, Society of Economic Geologists, Inc., 407-450. https://doi.org/10.5382/av100.14

[33] Fontaine, A., Eglinger, A., Ada, K., André-Mayer, A., Reisberg, L., Siebenaller, L., *et al.* (2017) Geology of the World-Class Kiaka Polyphase Gold Deposit, West African Craton, Burkina Faso. *Journal of African Earth Sciences*, **126**, 96-122. https://doi.org/10.1016/j.jafrearsci.2016.11.017

[34] Groves, D.I., Santosh, M., Zhang, L., Deng, J., Yang, L. and Wang, Q. (2021) Subduction: The Recycling Engine Room for Global Metallogeny. *Ore Geology Reviews*, **134**, Article ID: 104130. https://doi.org/10.1016/j.oregeorev.2021.104130

[35] Groves, D.I. and Santosh, M. (2023) Mineral Systems, Earth Evolution, and Global Metallogeny. Elsevier.

[36] Daigneault, R. (1991) Déformation et cisaillement: Concepts et applications. Ministère des Ressources Naturelles du Québec, DV89-16, 57 p.

[37] Nicolas, A. (1984) Principes de tectonique. Masson, 196 p.

[38] Lompo et Bamba (2010) Structures et minéralisations aurifères filoniennes dans les formations graphiteuses de Alga (Burkina Faso, Afrique de l'Ouest). *Journal of Science*, **10**, 1-12.

[39] Chardon, D., Bamba, O. and Traoré, K. (2020) Eburnean Deformation Pattern of Burkina Faso and the Tectonic Significance of Shear Zones in the West African Craton. *BSGF-Earth Sciences Bulletin*, **191**, Article No. 2. https://doi.org/10.1051/bsgf/2020001

[40] Passchier, C.W. and Trouw, R.A.J. (1998) Microtectonics. Springer-Verlag, 289 p.

[41] Velasquez, G., Beziat, D., Salvi, S., Siebenaller, L., Borisova, A.Y., Pokrovski, G.S., *et al.* (2013) Formation and Deformation of Pyrite and Implications for Gold Mineralization in the El Callao District, Venezuela. *Economic Geology*, **109**, 457-486. https://doi.org/10.2113/econgeo.109.2.457

[42] Traoré, Y.D., Siebenaller, L., Salvi, S., Béziat, D. and Bouaré, M.L. (2016) Progressive Gold Mineralization along the Syama Corridor, Southern Mali (West Africa). *Ore Geology Reviews*, **78**, 586-598. https://doi.org/10.1016/j.oregeorev.2015.11.003

[43] Ouedraogo, Y. (2021) Caractérisation de la déformation et de l'altération hydrothermale du gisement aurifère de Bissa, Burkina Faso, Afrique. Mémoire de Master, University JKZ.

[44] Cathelineau, M. (1988) Cation Site Occupancy in Chlorites and Illites as a Function of Temperature. *Clay Minerals*, **23**, 471-485. https://doi.org/10.1180/claymin.1988.023.4.13

[45] Beaudoin, G., Therrien, R. and Savard, C. (2006) 3D Numerical Modelling of Fluid Flow in the Val-d'Or Orogenic Gold District: Major Crustal Shear Zones Drain Fluids from Overpressured Vein Fields. *Mineralium Deposita*, **41**, 82-98. https://doi.org/10.1007/s00126-005-0043-5

[46] Mumin, A.H., Fleet, M.E. and Chryssoulis, S.L. (1994) Gold Mineralization in As-Rich Mesothermal Gold Ores of the Bogosu-Prestea Mining District of the Ashanti Gold Belt, Ghana: Remobilization of Invisible Gold. *Mineralium Deposita*, **29**, 445-460. https://doi.org/10.1007/bf00193506

[47] Hammond, N.Q. and Tabata, H. (1997) Characteristics of Ore Minerals Associated with Gold at the Prestea Mine, Ghana. *Mineralogical Magazine*, **61**, 879-894. https://doi.org/10.1180/minmag.1997.061.409.10

[48] Oberthür, T., Weiser, T., Amanor, J.A. and Chryssoulis, S.L. (1997) Mineralogical Siting and Distribution of Gold in Quartz Veins and Sulfide Ores of the Ashanti Mine and Other Deposits in the Ashanti Belt of Ghana: Genetic Implications. *Mineralium Deposita*, **32**, 2-15. https://doi.org/10.1007/s001260050068

[49] Allibone, A., Teasdale, J., Cameron, G., Etheridge, M., Uttley, P., Soboh, A., *et al.* (2002) Timing and Structural Controls on Gold Mineralization at the Bogoso Gold Mine, Ghana, West Africa. *Economic Geology*, **97**, 949-969. https://doi.org/10.2113/gsecongeo.97.5.949

[50] Lawrence, D.M., Treloar, P.J., Rankin, A.H., Harbidge, P. and Holliday, J. (2013) The Geology and Mineralogy of the Loulo Mining District, Mali, West Africa: Evidence for Two Distinct Styles of Orogenic Gold Mineralization. *Economic Geology*, **108**, 199-227. https://doi.org/10.2113/econgeo.108.2.199

[51] McCuaig, T.C., Fougerouse, D., Salvi, S., Siebenaller, L., Parra-Avila, L.A., Seed, R., *et al.* (2016) The Inata Deposit, Belahouro District, Northern Burkina Faso. *Ore Geology Reviews*, **78**, 639-644. https://doi.org/10.1016/j.oregeorev.2015.11.014

[52] Salvi, S., Velásquez, G., Miller, J.M., Béziat, D., Siebenaller, L. and Bourassa, Y. (2016) The Pampe Gold Deposit (Ghana): Constraints on Sulfide Evolution during Gold Mineralization. *Ore Geology Reviews*, **78**, 673-686. https://doi.org/10.1016/j.oregeorev.2015.11.006

[53] Masurel, Q., Miller, J., Hein, K.A.A., Hanssen, E., Thébaud, N., Ulrich, S., *et al.* (2016) The Yatela Gold Deposit in Mali, West Africa: The Final Product of a Long-Lived History of Hydrothermal Alteration and Weathering. *Journal of African Earth Sciences*, **113**, 73-87. https://doi.org/10.1016/j.jafrearsci.2015.10.006

[54] Ouedraogo, Y., Ilboudo, H., Ouiya, P., Toe, W.A.B. and Naba, S. (2025) Bissa Gold Mineralization in the Sabcé District, Goren Belt (Burkina Faso, West African Craton):

Implication of Arsenic in the Concentration of Visible and Invisible Gold in Pyrites. *Arabian Journal of Geosciences*, **18**, Article No. 51. https://doi.org/10.1007/s12517-025-12191-8

[55] Ouiya, P., Yaméogo, A.O., Ilboudo, H. and Naba, S. (2022) Implication of Paleoproterozoic Basalt Fertility Related to Mantle Plume Activity in Nassara Gold Mineralization (Burkina Faso, West Africa). *Open Journal of Geology*, **12**, 1013-1031. https://doi.org/10.4236/ojg.2022.1211048